System-Level Simulation for Homogeneous and Heterogeneous Cellular Networks

Nakrop Jinaporn, Simon Armour and Angela Doufexi
EPSRC Centre for Doctoral Training in Communications
University of Bristol
Bristol, UK
Email: {n.jinaporn, simon.armour, a.doufexi}@bristol.ac.uk

***Abstract*—To examine complex cellular networks, system-level simulation is one possible approach used by various radio planning tools. There is thus an opportunity to provide a comprehensive study including building blocks and simulation flow. In this article, the heterogeneous cellular network in downlink transmissions is simulated by means of system-level approach. Not only small cell deployments but also scheduling techniques are investigated in this simulation. The user throughput distribution is evaluated when varying the small cell placement, number of small cells and scheduling algorithms. Due to the use of small cells and proper scheduler, the user throughput could be significantly enhanced.**

***Index Terms*—Heterogeneous cellular networks, system-level simulation, long term evolution (LTE), scheduling**

I. Introduction

In a cellular network, there is a large number of network elements and associated links. To model such a network, simulation has been widely used before the real implementation. According to [1], this approach is likely to be classified into three types: link level (LL), system level (SL) and network level (NL) simulations.

A wireless link between a single transmitter and a single receiver is usually investigated by LL simulation. All functionalities of physical (PHY) and medium access control (MAC) layers are implemented. The block error rate (BLER) being an example of link performance indicators is evaluated. For SL simulation, a network consisting of a set of base stations and user terminals is modelled. The study of radio resource management (RRM) and interference coordination could be assisted by this SL simulation. To combine the effects from the LL into the SL, the link-to-system mapping has been performed [2]. For NL simulation, specific protocols and interfaces between layers are the focus of attention. Base stations are viewed as network entities which are able to exchange messages between each other.

In most mobile networks, radio planning and optimisation tools are required where there are both commercial and free simulators. Only existing SL software for long term evolution (LTE) networks is the focus of interest in this article. Firstly, ICS telecom [3] is one of commercial tools to model such networks. Some mobile features are provided such as network coverage, interference analysis, downlink (DL) and uplink (UL) throughput calculation, multiple-input and multiple-output (MIMO) and inter-system coexistence. This simulator is used globally by various institutions.

Another is the Vienna DL SL simulator [4]. This is a non-commercial simulator for academic use based on MATLAB designed to examine the radio access network (RAN) of LTE advanced (LTE-A) homogeneous and heterogeneous networks. Average wideband signal-to-interference-plus-noise ratio (SINR) and throughput being the example of performance metrics are obtained. Fortunately, the source code is permitted to be accessed by users resulting in scope for modification and potentially addition of new functionalities.

This article firstly aims to provide a review of SL simulation. Second, the SL simulation for LTE homogeneous and heterogeneous cellular networks in DL transmissions is developed using MATLAB. The building blocks and simulation flow are discussed step by step. Third, this developing simulator is used to analyse the effect of small cell deployments and scheduling techniques. The user throughput distribution is used for the performance evaluation under various network scenarios.

As compared with the existing article [5], the difference is the small cell placement. In [5], only the configuration of remote radio head (RRH) including cell ID is examined regardless of scheduling.

The remaining sections of this article are organized as follows: The SL simulation is described in Sec. II. Subsequently, the simulation results are presented in Sec. III. Finally, a summary of the article and future works are concluded in Sec. IV.

II. System-Level Simulation

In this section, the building blocks of SL simulation for LTE homogeneous and heterogeneous networks in DL are described. Simulation flow and performance metrics are also discussed. For the modelling method, the pre-generated data such as fading loss from Sec. II-A to II-D are first required. Then, these data will be used in the main simulation loop in Sec. II-E and post-processing in Sec. II-F.

A. Building Blocks

1) Network Layout: According to [6], a hexagonal grid of 19 sites with three sectors is firstly generated as shown in Fig. 1. This homogeneous network results in 57 sectors in total. Only the region of interest (ROI) is investigated (e.g.,

a rectangle of approximately 2000 $\times$ 1732 m) for the SL simulation. This area is defined by the site positions at the border. Meanwhile, the ROI can be expanded by an increasing factor for different interference modelling.

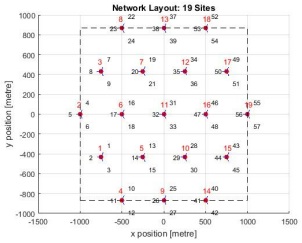

Fig. 1. The tri-sectorised hexagonal cell layout (19 sites, 3 sectors per site).

The ROI can be considered as a (2 dimensional) pixel map with a given resolution of p m/pixel. The large-scale fading including pathloss, antenna gain and shadow fading can be stored on each pixel of $p \times p$ m.

Unlike the homogeneous cellular network, a mixture of existing macro network and indoor femtocells can be employed in a heterogeneous network. In [4], there are two possible models for femtocell placement including homogeneous density and a fixed number of femtocells per macro sector. Fig. 2 shows the femtocell placement resulting from the former model. 33 femto sites (green dots) are uniformly placed over the ROI of approximately 3.3 km^2 with an average density of 10 femtocells/km^2.

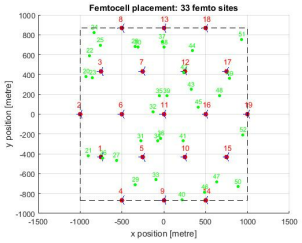

Fig. 2. Femtocell placement.

2) Antenna Gain: The antenna gain based on [6], [7] is deployed. The base station (or eNB) antenna pattern (horizontal) for each macro sector (in dB) is given by

$$A_{\mathrm{H}}(\theta) = -\min\left[12\left(\frac{\theta}{\theta_{3\mathrm{dB}}}\right)^2, A_{\mathrm{m}}\right], \tag{1}$$

where $-180^\circ \leq \theta \leq 180^\circ$. Let $\theta_{3\mathrm{dB}}$ and A_{m} be the 3dB beamwidth and the maximum attenuation, respectively. $\theta_{3\mathrm{dB}} = 65^\circ$ and $A_{\mathrm{m}} = 15$ dB are set. Thus, the transmit antenna gain of eNB for any user equipment (UE) is computed (in dB)

$$G_{\mathrm{TX}} = G_{\mathrm{m}} + A(\theta), \tag{2}$$

where the maximum base station antenna gain G_{m} = 15 dBi. For femtocells, the antenna pattern (horizontal) is assumed to be omnidirectional ($A_{\mathrm{H}}(\theta) = 0$ dB).

3) Pathloss: For a homogeneous network, the pathloss model (in dB) is defined as [6]

$$L(R) = 128.1 + 37.6\log_{10}(R), \tag{3}$$

where R is the separation distance between transmitter and receiver (in km). A carrier frequency of 2000 MHz and an eNB antenna height of 15 metres above the average rooftop level are used in (3).

If a heterogeneous scenario is also considered, the pathloss model of femto to UE links is then expressed [8]

$$L(R) = 127 + 30\log_{10}(R). \tag{4}$$

This simplified model is used for a femto site and its UEs without any walls. For other links, the model from (3) is applied to the communication between a UE and other femto and macro sites.

By combining antenna gain, pathloss and minimum coupling loss (MCL)[1], the large-scale fading map for a given macro sector (transmitter) can be visualised in Fig. 3.

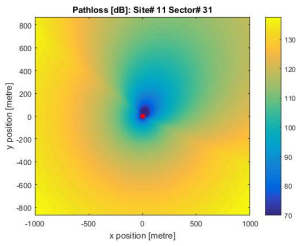

Fig. 3. Pathloss and antenna gain map (in dB) for a macro sector.

4) Shadow Fading: Shadowing is typically modelled according to a log-normal distribution, i.e., as the normal random variable with zero mean and a standard deviation of 10 dB [6]. Due to the mobility of eNBs or UEs, the spatial correlation of shadow fading values needs to be considered in the modelling. The normalised correlation function can be expressed

$$r(x) = e^{-\alpha x}, \tag{5}$$

where x denotes a separation distance between two points and $x \geq 0$. A value of $\alpha = 1/20$ has been recommended for a scenario between urban and suburban deployments.

For the conventional approach, correlated shadow fading values (s) are generated as follows

$$\mathbf{s} = \mathbf{L}\mathbf{a}, \tag{6}$$

where $\mathbf{a}$ is an uncorrelated shadow fading vector with $\mathbb{E}\{\mathbf{a}\mathbf{a}^{\mathrm{T}}\} = \mathbf{I}$. Each element in $\mathbf{a}$ is generated (in dB) as a normal random variable. The correlation matrix of $\mathbf{s}$ is

[1]It is defined as the minimum signal loss between the network elements in the worse case: 70 dB for urban and 80 dB for rural area scenarios [6]. This leads to $P_{\mathrm{RX}} = P_{\mathrm{TX}} - \mathrm{Max}(L(R) - G_{\mathrm{TX}} - G_{\mathrm{RX}}, \mathrm{MCL})$. Let $P_{\mathrm{RX}}, P_{\mathrm{TX}}$ and G_{RX} be the received signal power, transmitted signal power and receiver antenna gain, respectively.

$\mathbf{R} = \mathbb{E}\{\mathbf{s}\mathbf{s}^{\mathrm{T}}\} = \mathbf{L}\mathbf{L}^{\mathrm{T}}$ where $\mathbf{L}$ is the Cholesky decomposition of $\mathbf{R}$.

To decrease the computational complexity, spatially correlated shadowing values are generated in connection with the neighboring pixels in the map [9]. For instance, only four neighboring values are used for the correlation operation. A vector of correlated shadowing values $\tilde{\mathbf{s}} = (s_1, s_2, s_3, s_4)^{\mathrm{T}}$ with $\tilde{\mathbf{R}} = \mathbb{E}\{\tilde{\mathbf{s}}\tilde{\mathbf{s}}^{\mathrm{T}}\}$ can be extended to $\mathbf{s} = (s_1, s_2, s_3, s_4, s_{\mathrm{n}})^{\mathrm{T}}$ with $\mathbf{R} = \mathbb{E}\{\mathbf{s}\mathbf{s}^{\mathrm{T}}\}$. Each element in $\tilde{\mathbf{R}}$ and $\mathbf{R}$ is computed using (5).

By doing this, the condition (6) can be modified

$$\begin{aligned} \mathbf{s} &= \mathbf{L}\mathbf{a} \\ &= \mathbf{L}\begin{bmatrix} \tilde{\mathbf{L}}^{-1}\tilde{\mathbf{s}} \\ a_{\mathrm{n}} \end{bmatrix}. \end{aligned} \tag{7}$$

Therefore, the new correlated shadow fading value can be obtained

$$s_{\mathrm{n}} = \lambda_{\mathrm{n}}^{\mathrm{T}}\begin{bmatrix} \tilde{\mathbf{L}}^{-1}\tilde{\mathbf{s}} \\ a_{\mathrm{n}} \end{bmatrix}, \tag{8}$$

where a_{n} is the generated normal random variable and $\lambda_{\mathrm{n}}^{\mathrm{T}}$ is the last row of $\mathbf{L}$. In addition, an inter-site correlation of 0.5 and inter-sector correlation of one are assumed to generate $\mathbf{a}$ [6]. Fig. 4 shows the shadow fading map with 4 neighbouring correlation matrices. Note that a single map per site is generated in this simulation. The same method is used for all macro and femto sites.

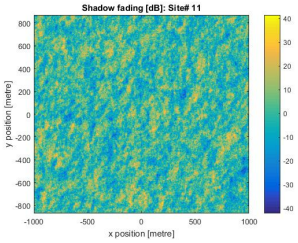

Fig. 4. Shadow fading map (in dB) for the (macro) site number 11.

B. Wideband SINR

For the cell partitioning, the wideband SINR (geometry) of the strongest signal on each pixel is determined

$$\Gamma = \frac{G_{\mathrm{TX},0} \cdot L_{\mathrm{M},0} \cdot P_{\mathrm{TX},0}}{\sigma_{\mathrm{n}}^2 + \sum_{l=1}^{N_{\mathrm{int}}} G_{\mathrm{TX},l} \cdot L_{\mathrm{M},l} \cdot P_{\mathrm{TX},l}}, \tag{9}$$

where $L_{\mathrm{M},i}$ is the large-scale fading loss (the index $i = 0$ for the desired transmitter and $i = 1, \ldots, N_{\mathrm{int}}$ for the interfering transmitters) and σ_{n}^2 is the receiver noise power. If only pathloss is considered as $L_{\mathrm{M},i}$, the wideband SINR for a macro-femto case can be visualised in Fig. 5.

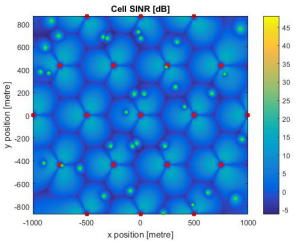

Fig. 5. Wideband SINR (in dB) for a macro-femto scenario.

C. User Distribution

Due to the known wideband SINR, the strongest signal on each pixel can be obtained. The sector which provides the maximum SINR is assigned (identified) to that pixel. Then, all possible pixels of a serving sector on the map will be determined. For the UE distribution, the constant number of UEs per sector is set. Subsequently, a set of UEs is randomly located within the pixels of their serving sector. For example, there are 10 possible pixels and 2 attached UEs of a specific sector. In this way, only two of ten positions are randomly selected for the attached UEs while the remaining locations are not placed by any UEs. Note that UEs are not generated for some unassigned sectors.

Fig. 6 shows as example of this UE distribution for the case of 2 UEs per macro sector and 1 UE per femto sector. There are 53 macro sectors and 33 femto sectors which are assigned. This results in the 139 UEs (blue diamond markers) being generated. Note that larger numbers of UEs will be used for meaningful simulations but that this case serves as a good illustrative example.

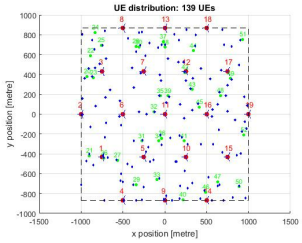

Fig. 6. User distribution for a macro-femto scenario.

D. Small-Scale Fading

Small-scale fading can be pre-generated based on power delay profile (PDP). Moreover, correlated fading could be involved with this fading generation. A variety of PDPs can be selected such as ITU pedestrian (A and B), extended pedestrian B, vehicular (A and B) and typical urban (TU) channels.

After obtaining the PDP, the next step is to generate the Rayleigh fading channel coefficient. A simple way is described in [10], [11] where both in-phase (X_I) and quadrature (X_Q) are two (uncorrelated) Gaussian random variables with zero mean and equal variance (σ^2). These two components are independent.

Another method for (correlated) fading generation is proposed in [12]. This improved work stems from the well-known Clarke and Jake's reference model. The randomness for random path gain (C_n), angle of incoming wave (α_n) and initial phase (ϕ_n) corresponding to the nth path is reintroduced. Owing to the page limit, the complete procedure could be found in [12].

E. Main Simulation Loop

According to [4], the main simulation loop can be described. The simulation will be repeated until reaching the configured simulation duration. For each iteration, there are six stages as follows:

1) Place/move UEs
   - The initial UE positions for the first transmission time interval (TTI) are obtained from the pre-computed UE distribution in Fig. 6.
   - UE positions are randomly generated (e.g., a walking model).
   - UE positions from previous TTI are used to define current UE positions.
2) Link quality model
   - Current UE positions are applied to obtain the pre-computed large-scale fading from the pixel map.
   - Current TTI is used to select the pre-generated small-scale fading for each UE.
   - UE information such as transmission mode, resource block (RB) grid and power allocation is specified.
   - Received (post-equalisation) SINRs and channel quality indicator (CQI) feedback are determined [13].
3) eNBs receive and process the feedback from UEs
   - The availability of UE feedback at eNB is identified.
   - Current feedback is recorded in the feedback buffer for the next TTI.
4) eNBs schedule transmissions to the UEs
   - RB allocation (e.g., round-robin, best-CQI and proportional fair).
   - Power allocation (e.g., homogeneous manner).
   - eNB signaling (e.g., CQI, transport block (TB) size and assigned RBs).
5) Link performance model
   - The information from link quality model (post-equalisation SINR) and scheduling stages (eNB signaling) is imported.
   - TB SINR, BLER and acknowledgment (ACK) are determined, if any RBs are assigned.
   - The feedback such as BLER and ACK is updated.
6) Update the UE feedback to the channel
   - Related feedback is stored in the buffer for post-processing and the following TTIs.

F. Post-Processing

After the main loop is terminated, the simulation results from each iteration (TTI) are processed resulting in UE and system performance metrics. For example, the average throughput of a given UE (in Mbps) can be calculated [4]

$$T_{\text{avg}} = \frac{B_{\text{total}}}{N_{\text{TTI}} \times L_{\text{TTI}} \times 10^6}, \tag{10}$$

where the total bit $B_{\text{total}} = \sum_{i \in A}(\text{ACK}_i \times \text{TB}_{\text{size},i})$. Let ACK_i and $\text{TB}_{\text{size},i}$ be the acknowledgment and the transport block size (in bits) on the TTI ith, respectively. Denote the set and number of accounted TTIs by A and N_{TTI}, respectively. The TTI without feedback information is not investigated. The TTI length (L_{TTI}) of 1 ms is fixed.

III. Performance Evaluation

The results from homogeneous and heterogeneous cases are presented in this section. The simulation has been performed by MATLAB in connection with the methodology in Sec. II. This simulator uses separate MATLAB functions instead of object-oriented programming (OOP) approach in the Vienna simulator [4]. Different network element placement methods and scheduling algorithms are used.

A. Simulation Parameters

The simulation parameters for macro sites and femtocells are shown in Tab. I - II. Some parameters are the same for both cases. Note that only femtocells and (macro and femto) UEs within the specific area corresponding with the central macro site are used for this simulation. To consider the randomness of femtocell location, all femto sites are randomly placed in each TTI. In this way, the number of femtocells and femto UEs may be varied.

TABLE I
Simulation parameters (macro network)

Parameter	**Assumption**
Cellular layout	Hexagonal grid of 19 sites
Inter-site distance	500 m
Path loss model	$L = 128.1 + 37.6 \log_{10}(R)$
Lognormal shadow fading	$L_s \sim N(\mu, \sigma^2)$
Shadowing mean	0 dB
Shadowing standard deviation	10 dB
Antenna pattern (horizontal)	$A_{\text{H}}(\theta) = -\min\left[12\left(\frac{\theta}{\theta_{\text{3dB}}}\right)^2, A_{\text{m}}\right]$
Carrier frequency	2.14 GHz
System bandwidth	1.4 MHz
Channel model	ITU Pedestrian A model
UE speed	5 km/h
Number of UEs	30 UEs per sector
Total BS TX power (P_{total})	46 dBm
Scheduling	Round-robin and best-CQI
Transmission mode	Single-input single-output (SISO)
Simulation length	50 TTIs

TABLE II
SIMULATION PARAMETERS (FEMTOCELL NETWORK)

Parameter	Assumption
Cellular layout	Random placement
Inter-site distance	N/A
Path loss model	$L = 127 + 30\log_{10}(R)$
Antenna pattern (horizontal)	$A_{\mathrm{H}}(\theta) = 0$ dB
Number of UEs	2 UEs per sector
Total BS TX power (P_{total})	20 dBm

B. UE Throughput Distribution

Based on (10), the average UE throughput could be determined for the macro and macro-femto scenarios. The empirical cumulative distribution function (ecdf) of UE throughput when varying the homogeneous density (10 and 20 femtocells/km^2) and a constant femtocell per macro sector (1 and 2 femtocells per sector) is presented in Fig. 7. All results are compared with the macro scenario under the round-robin scheduling.

Due to the femtocell deployment, some performance metrics could be enhanced, in particular peak throughput (the 95% point of the UE throughput ecdf). For example, the peak throughput in the case of 2 femtocells per sector (magenta solid line) was around eight times as large as the macro scenario (black solid line).

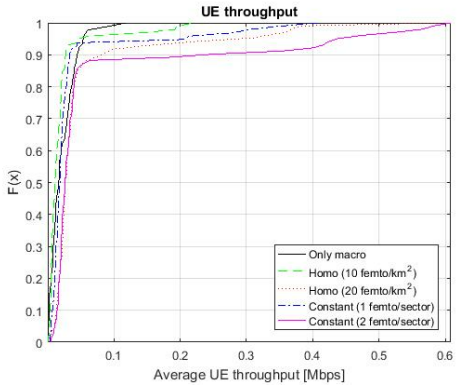

Fig. 7. The ecdf of UE throughput (round-robin scheduling).

Fig. 8 shows the ecdf of UE throughput under the round-robin and best-CQI approaches. Because of the latter scheduler, the peak throughput was increased for both macro and macro-femto (2 femtocells per sector) cases. A specific RB was allocated to the UE with the maximum CQI. However, there was the expense of edge throughput and fairness as compared with the round-robin manner. Not only small cell deployments but also efficient scheduling techniques are required to enhance the system performance.

IV. DISCUSSION AND CONCLUSIONS

In this article, the SL simulation for cellular networks was the main focus of attention. Building blocks such as network layout, large-scale fading and small-scale fading were described. The simulation flow was also indicated. Subsequently, the simulation for LTE homogeneous and heterogeneous deployments in DL transmissions was performed to evaluate the distribution of UE throughput. The enhanced peak throughput could be obtained from the femtocell deployments and best-CQI scheduler. Open challenges include: how the SL simulation can be implemented in connection with scheduling, carrier aggregation and unlicensed spectrum use and beyond LTE link level technologies.

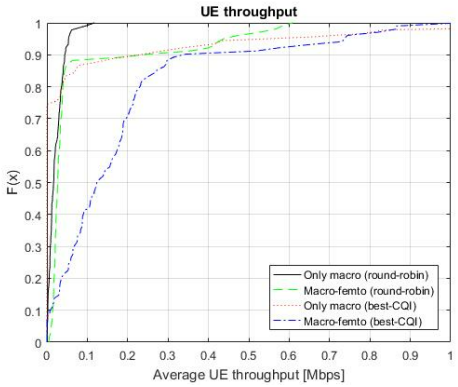

Fig. 8. The ecdf of UE throughput (round-robin and best-CQI schedulers).

REFERENCES

[1] P. Alvarez, C. Galiotto, J. van de Belt, D. Finn, H. Ahmadi, and L. DaSilva, "Simulating dense small cell networks," in *2016 IEEE Wireless Communications and Networking Conference*. IEEE, apr 2016, pp. 1–6.

[2] K. Brueninghaus, D. Astely, T. Salzer, S. Visuri, A. Alexiou, S. Karger, and G. Seraji, "Link Performance Models for System Level Simulations of Broadband Radio Access Systems," in *2005 IEEE 16th International Symposium on Personal, Indoor and Mobile Radio Communications*, vol. 4. IEEE, 2005, pp. 2306–2311.

[3] ATDI, "ICS telecom EV." [Online]. Available: http://www.atdi.com/ics-telecom/

[4] M. Rupp, S. Schwarz, and M. Taranetz, *The Vienna LTE-advanced simulators : up and downlink, link and system level simulation*, 1st ed. Springer Singapore, 2016.

[5] X. Wang, Y. Chen, and Z. Mai, "A Novel Design of System Level Simulator for Heterogeneous Networks," in *2017 IEEE Globecom Workshops (GC Wkshps)*. IEEE, dec 2017, pp. 1–6.

[6] 3GPP, "LTE; Evolved Universal Terrestrial Radio Access (E-UTRA); Radio Frequency (RF) system scenarios (3GPP TS 36.942 version 13.0.0 Release 13)," 3GPP, Tech. Rep., 2016.

[7] ——, "3GPP TSG RAN WG4 (Radio) Meeting #51: Simulation assumptions and parameters for FDD HeNB RF requirements," 3GPP, San Francisco, Tech. Rep., 2009.

[8] ——, "Evolved Universal Terrestrial Radio Access (E-UTRA); Further advancements for E-UTRA physical layer aspects (3GPP TR 36.814 version 9.1.0 Release 9)," 3GPP, Tech. Rep., 2016.

[9] H. Claussen, "Efficient modelling of channel maps with correlated shadow fading in mobile radio systems," in *2005 IEEE 16th International Symposium on Personal, Indoor and Mobile Radio Communications*, vol. 1. IEEE, 2005, pp. 512–516.

[10] T. S. Rappaport, *Wireless communications : principles and practice*, 2nd ed. Prentice Hall PTR, 2002.

[11] A. Goldsmith, *Wireless communications*. Cambridge University Press, 2005.

[12] Y. Zheng and Chengshan Xiao, "Simulation models with correct statistical properties for rayleigh fading channels," *IEEE Transactions on Communications*, vol. 51, no. 6, pp. 920–928, jun 2003.

[13] J. C. Ikuno, M. Wrulich, and M. Rupp, "System Level Simulation of LTE Networks," in *2010 IEEE 71st Vehicular Technology Conference*. IEEE, 2010, pp. 1–5.